


RESEARCH ARTICLE | MAY 01 2023

Recombination of vibrationally cold N_2^+ ions with electrons

L. Uvarova; S. Rednyk; P. Dohnal ; ... et. al



J. Chem. Phys. 158, 174303 (2023)

<https://doi.org/10.1063/5.0149110>



CrossMark

Articles You May Be Interested In

Piezoelectric single crystal and magnetostrictive Metglas composites: Linear and nonlinear magnetoelectric coupling

Appl. Phys. Lett. (April 2014)

Effect of Large Vacancy Thermal Expansion on the Pressure Variation of Activation Enthalpy in Pure Metals

Journal of Applied Physics (November 2003)

High magnetoelectric tuning effect in a polymer-based magnetostrictive-piezoelectric laminate under resonance drive

Journal of Applied Physics (March 2012)



Time to get excited.
Lock-in Amplifiers – from DC to 8.5 GHz



[Find out more](#)

 Zurich
Instruments

Recombination of vibrationally cold N_2^+ ions with electrons

Cite as: J. Chem. Phys. 158, 174303 (2023); doi: 10.1063/5.0149110

Submitted: 3 March 2023 • Accepted: 17 April 2023 •

Published Online: 1 May 2023



View Online



Export Citation



CrossMark

L. Uvarova,¹ S. Rednyk,¹ P. Dohnal,^{1,a)} M. Kassayová,¹ S. Saito,² Š. Roučka,¹ R. Plašil,¹
R. Johnsen,³ and J. Glosík¹

AFFILIATIONS

¹ Faculty of Mathematics and Physics, Department of Surface and Plasma Science, Charles University, Prague, Czech Republic

² Department of Physics, Rikkyo University, Tokyo, Japan

³ Department of Physics and Astronomy, University of Pittsburgh, Pittsburgh, Pennsylvania 15260, USA

^{a)} Author to whom correspondence should be addressed: petr.dohnal@mff.cuni.cz

ABSTRACT

Recombination of vibrationally cold N_2^+ ions with electrons was studied in the temperature range of 140–250 K. A cryogenic stationary afterglow apparatus equipped with cavity ring-down spectrometer and microwave diagnostics was utilized to probe *in situ* the time evolutions of number densities of particular rotational and vibrational states of N_2^+ ions and of electrons. The obtained value of the recombination rate coefficient for the recombination of the vibrational ground state of N_2^+ with electrons is $\alpha_{v=0} = (2.95 \pm 0.50) \times 10^{-7} (300/T)^{(0.28 \pm 0.07)} \text{ cm}^3 \text{ s}^{-1}$, while that for the first vibrationally excited state was inferred as $\alpha_{v=1} = (4 \pm 4) \times 10^{-8} \text{ cm}^3 \text{ s}^{-1}$ at 250 K.

Published under an exclusive license by AIP Publishing. <https://doi.org/10.1063/5.0149110>

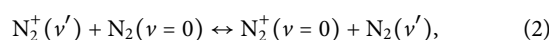
I. INTRODUCTION

Molecular nitrogen is the most abundant gas in the Earth atmosphere and also a major component of the atmospheres of other solar system bodies such as Pluto,¹ Titan,² or Triton.³ It is one of the main species in ices covering surfaces of trans-Neptunian objects.⁴ As a result, N_2^+ is a main molecular ion in the Earth atmosphere⁵ as well as in the atmospheres of Titan⁶ and Triton.⁷ It is also an important element in many technical and industrial processes^{8–11} and in nitrogen containing plasmas. Dissociative recombination of N_2^+ ions with electrons,



is a key process in ionospheric modeling^{12–14} and has been for more than 70 years subject of many theoretical and experimental studies (for details see reviews).^{13,15,16} The reported recombination rate coefficients differ by a factor of two to three. This has clear implications for our ability to understand observed electron density profiles¹⁷ or for the studies focused on the composition of the lower ionosphere.¹⁸ Moreover, the temperature dependence of the recombination rate coefficients can also substantially affect the ionospheric composition¹⁹ and ionospheric instabilities.^{20,21}

Deionization of a nitrogen plasma was studied in a seminal work by Biondi and Brown²² that served as stimulus for Bates to develop his theory of dissociative recombination.²³ These early experiments were performed without identification of recombining ions and were characterized by strong pressure dependences of the measured recombination rate coefficients. The Biondi *et al.*^{24,25} added mass spectrometry to their stationary afterglow setup and reported values of recombination rate coefficient for N_2^+ at 300 K of $2.9 \times 10^{-7} \text{ cm}^3 \text{ s}^{-1}$ and later $1.8 \times 10^{-7} \text{ cm}^3 \text{ s}^{-1}$. The actual vibrational population of the recombining ions was not known. Zipf²⁶ using laser induced fluorescence and similar conditions as those in Biondi's experiments reported 87% of all N_2^+ ions in the ground vibrational state with the inferred value of the recombination rate coefficient for $N_2^+(v=0)$ being $2.2 \times 10^{-7} \text{ cm}^3 \text{ s}^{-1}$ and higher for $v=1$ and $v=2$ states. Johnsen²⁷ pointed out that the analysis of Zipf's data did not take into account the efficient resonant charge exchange process between N_2^+ ions and nitrogen molecules,



and that the measured recombination rate coefficient reflected the high vibrational temperature (~ 1500 K) of the N_2^+ ions. Bates

and Mitchell²⁸ reanalyzed Zipf's data with the inclusion of the charge exchange process (2) and suggested a corrected value of $2.6 \times 10^{-7} \text{ cm}^3 \text{ s}^{-1}$ for the vibrational ground state of N_2^+ at 300 K. The reanalysis also indicated that the value of the recombination rate coefficient would decrease with increasing vibrational excitation of the N_2^+ ions.

The FALP (Flowing Afterglow with Langmuir Probe) experiments by Mahdavi *et al.*, Geoghegan *et al.*,^{29,30} and Canosa *et al.*³¹ reported values of the recombination rate coefficient for N_2^+ ions at room temperature of 2.2×10^{-7} , 2.0×10^{-7} and $2.6 \times 10^{-7} \text{ cm}^3 \text{ s}^{-1}$, respectively. The advantage of the FALP technique in comparison with stationary afterglow is that the studied ions are produced separately from the discharge and are thus with high probability in their vibrational ground state.

Cunningham and Hobson³² used a shock tube to measure the temperature dependence of the recombination rate coefficient for the N_2^+ ions in the range of 700–2700 K. Despite the high temperatures used in the study, they claimed that the obtained results are for $\nu = 0$ state of N_2^+ and by extrapolating their data down to 300 K got value of $\alpha = 1.78 \times 10^{-7} \text{ cm}^3 \text{ s}^{-1}$. Mul and McGowan³³ used the single-pass merged electron-ion beam technique and obtained the dependence of the recombination rate coefficient $\alpha = 3.6 \times 10^{-7} (T_e/300 \text{ K})^{(-0.5)} \text{ cm}^3 \text{ s}^{-1}$ for electron temperatures between 100 and 20 000 K (according to Refs. 16 and 34 this value should be divided by a factor of two due to calibration error). The internal excitation of the recombining ions was not known. In another single-pass merged electron-ion beam study, Noren *et al.*³⁵ employed a Radio frequency ion trap source that could be utilized to control the number of collisions that the ions undergo prior to their injection to the beam line. The obtained value of the recombination rate coefficient for vibrationally cold ions was $0.4 \times 10^{-7} \text{ cm}^3 \text{ s}^{-1}$, substantially lower than values reported in afterglow experiments, and increased when number of collisions in the ion source decreased—i.e., for vibrationally excited ions. Sheehan and St.-Maurice¹³ in their excellent review speculated that instead of vibrational quenching, the ions became vibrationally reactivated due to collisions in the ion source. On the other hand, Florescu-Mitchell and Mitchell¹⁵ suggested that possible calibration error could explain results of Noren *et al.*³⁵

The single-pass merged electron-ion beam study of Sheehan and St.-Maurice¹³ and the ion storage ring experiment CRYRING³⁶ reported practically identical cross sections for recombination of N_2^+ ions with electrons in a broad energy range. The corresponding recombination rate coefficients for the temperature of 300 K were 1.5×10^{-7} and $1.75 \times 10^{-7} \text{ cm}^3 \text{ s}^{-1}$, respectively. The latter study also probed vibrational populations of the recombining ions with 46% percent of all N_2^+ ions in the $\nu = 0$ state, 27% in $\nu = 1$, 10% in $\nu = 2$, and 16% in $\nu = 3$ state.

Despite the breadth of the available experimental data, the reported values of recombination rate coefficients differ by a factor of two or more at 300 K and there are no experiments with vibrationally cold ions performed for temperatures below 300 K. The majority of the studies, with notable exception of single-pass merged electron-ion beam experiment by Noren *et al.*,³⁵ also hint that the recombination rate coefficient decreases with increasing vibrational excitation of the recombining ions (for further discussion see Ref. 13). Unfortunately, of all the studies that were able to determine the vibrational populations of the recombining N_2^+ ions, none was

conducted with overwhelming majority of ions in the vibrational ground state.

Dissociative recombination of N_2^+ ions with electrons was extensively theoretically studied by Guberman^{37–41} using multichannel quantum defect approach (MQDT). His calculations have shown that at elevated temperatures the $\nu = 0$ state of N_2^+ will recombine with electrons faster than the excited states. At 300 K the predicted ratio between the values of the recombination rate coefficients for the two lowest vibrational states of N_2^+ is < 1.5 and decreasing with decreasing temperature.

Little *et al.*⁴² used the framework of the R matrix theory to obtain the recombination rate coefficients for several low lying vibrational states of N_2^+ . This approach was later refined by Abdoulanziz *et al.*⁴³ by taking into account higher kinetic energies of incoming electrons and more vibrational levels of the target molecular ion. Their calculations confirmed Guberman's results⁴¹ that $\nu = 0$ state of N_2^+ recombines faster than the vibrationally excited states but the ratio between recombination rate coefficients for $\nu = 0$ and $\nu = 1$ states is predicted to be more than 4 at the temperature of 300 K and does not significantly change with decreasing temperature. The obtained absolute value of the recombination rate coefficient for $\nu = 0$ is also higher than that from MQDT theory⁴¹ while the value for the $\nu = 1$ state is substantially lower.

In this paper, we present the results of experimental study on recombination of the vibrational ground state of N_2^+ ions with electrons performed in the temperature range of 140–250 K. In contrast to previous studies, the time evolutions of number densities of different rotational and vibrational states of N_2^+ and of electrons were probed *in situ* at temperatures below 300 K. Moreover, the used experimental technique enables reliable recombination rate coefficient determination even at conditions where the studied ions are not dominant ionic specie in afterglow plasma.

II. EXPERIMENT

A Cryogenic Stationary Afterglow apparatus with Cavity Ring Down Spectrometer (Cryo-SA-CRDS) was used in the present experiments. The simplified scheme of the experimental setup is shown in Fig. 1 and its detailed description can be found e.g., in Refs. 44 and 45 so only a short overview will be given here. The gas of the required composition enters the discharge tube on one side and is pumped by a roots pump on the other side. The plasma is produced in a sapphire discharge tube with an inner diameter of 2.2 cm and a length of 20 cm by a microwave discharge in a prepared gas mixture. The discharge tube is cooled by a closed cycle helium refrigerator enabling operation in the temperature range of 30–300 K. The Cavity Ring-Down Spectrometer based on an approach developed by Romanini *et al.*⁴⁶ is used to monitor the time evolutions of the number densities of ions, in particular, rotational (and vibrational) state. The optical cavity consists of two highly reflective plano-concave mirrors with a reflectivity greater than 99.99%. The light that leaves the cavity through the second mirror is detected by an InGaAs avalanche photodiode. For the experiment with N_2^+ ions, we used an optical system consisting of two lasers (L785P090 with central wavelength of 785 nm and L808P030 centered at 808 nm) covering transitions in the Meinel system of $\text{N}_2^+ \text{ } ^2\Sigma_g^+ \text{ } ^2\Pi_u$ originating in the ground and the first vibrational state of the ion. The transitions

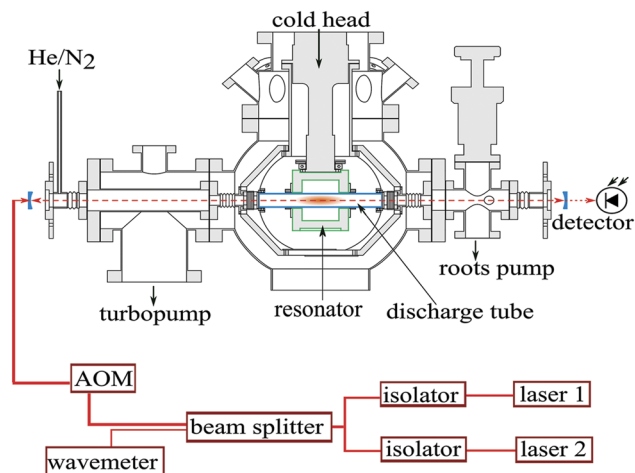


FIG. 1. A scheme of the Cryogenic Stationary Afterglow with Cavity Ring-Down Spectrometer (Cryo-SA-CRDS) apparatus. The microwave resonator (green in the figure) is connected to the discharge tube via copper braids. A cold head of the closed cycle helium refrigerator Sumitomo RDK 408S is attached to the microwave resonator enabling operating the discharge tube in the temperature range of 30–300 K. The laser is switched on and off by passing through an acousto-optic modulator (AOM) and then passes through mode matching optics (not in the figure) before entering the optical cavity formed by two highly reflective plano-concave mirrors. The light leaking through the cavity is collected on a detector consisting of an avalanche photodiode and amplifier.

used in the present study are listed in Table I. The Einstein A coefficients for transitions between different vibronic levels were taken from Ref. 47 and the state to state line intensities were calculated following Refs. 48 and 49 using Hönl-London factors from Ref. 50, spectroscopic constants from Ref. 51 and transition wavenumbers published in Refs. 51 and 52. The wavelength is measured absolutely by WA-1650 wavemeter.

The time evolution of the electron number density in the afterglow plasma is determined by tracing the changes in the resonant frequency of the microwave resonator. For details, see Ref. 45. The N_2^+ ions are formed in a pulsed microwave discharge (10 W, period of 3 ms, discharge on for few hundred μ s) ignited in a He/ N_2 mixture with a typical composition of $10^{17}/10^{14}$ cm^{-3} . The buffer gas flow is measured by mass flow meter positioned on the inlet gas tube. The typical gas flow velocity at the center of the discharge tube is on the order of 1 m s^{-1} and the used gases are purified prior to entering the discharge tube by passing through liquid nitrogen cold traps. Our previous studies,^{44,45} performed in the temperature range of 30–200 K, have shown that for H_3^+ ions in helium buffer gas the kinetic T_{kin} temperature of the ions in the discharge tube is within the error of the measurement equal to the temperature given by the temperature sensor positioned on the stainless-steel holder of the discharge tube.

III. DATA ANALYSIS

The values of the recombination rate coefficients were obtained from the measured time evolutions of the electron and ion number densities using the procedure described in detail by Shapko *et al.*⁴⁵

TABLE I. List of transitions of the ${}^2\Sigma_g^+ - {}^2\Pi_u$ Meinel system of N_2^+ used in present study. v'' and v' denote the vibrational quantum number of the lower and upper state, respectively. The transition wavenumbers ν were taken from Ref. 51 for transitions originating in the ground vibrational state of N_2^+ and from Ref. 52 for the $v = 1$ state. For details on spectroscopic notation see Ref. 51. Lines denoted by asterisk were overlapping to some degree with nearby lines of N_2 .

Transition	v''	v'	ν (cm^{-1})
$R_{11}(8.5)$	1	3	12 358.082
$R_{11}(9.5)$	1	3	12 358.354
$Q_{22}(11.5)$	1	3	12 358.426
$Q_{22}(9.5)$	1	3	12 370.692*
$Q_{21}(18.5)$	1	3	12 374.848*
$Q_{22}(10.5)$	0	2	12 726.047*
$P_{21}(10.5)$	0	2	12 731.879
$Q_{22}(9.5)$	0	2	12 731.981
$R_{22}(17.5)$	0	2	12 737.000
$P_{21}(9.5)$	0	2	12 737.428
$Q_{22}(8.5)$	0	2	12 737.524
$P_{21}(8.5)$	0	2	12 742.591
$Q_{22}(7.5)$	0	2	12 742.675
$P_{22}(3.5)$	0	2	12 747.298*
$P_{21}(7.5)$	0	2	12 747.370
$Q_{22}(6.5)$	0	2	12 747.436

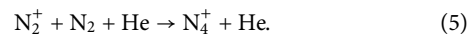
If N_2^+ ions are no longer formed in the afterglow plasma, the time evolution of their number density can be described by the formula

$$\frac{dn_{N_2^+}}{dt} = -\alpha n_{N_2^+} n_e - \frac{n_{N_2^+}}{\tau}, \quad (3)$$

where $n_{N_2^+}$ and n_e are the number densities of N_2^+ ions and of electrons, α is the recombination rate coefficient, and τ is the time constant for the losses of N_2^+ ions by ambipolar diffusion and by reactions (ion-molecule reaction, three-body association reaction, etc.):

$$\frac{1}{\tau} = \frac{1}{\tau_D} + \frac{1}{\tau_R}, \quad (4)$$

where τ_D is the time constant of ambipolar diffusion losses and τ_R describes reaction losses. At conditions in the present experiments (temperature, pressure, reactant number density), this term is given mainly by the formation of N_4^+ ions in the three-body association reaction of N_2^+ with N_2 and He:



The value of the rate coefficient for reaction (5) was determined by Anichich *et al.*⁵³ to be $2 \times 10^{-29} \text{ cm}^3 \text{ s}^{-1}$ at 300 K.

By directly integrating Eq. (3), we get the N_2^+ number density in time t_1 in the afterglow:

$$n_{N_2^+}(t_1) = n_{N_2^+}(t_0) e^{-\alpha X(t_1) - \frac{t_1}{\tau}}, \quad (6)$$

where $n_{N_2^+}(t_0)$ is the initial number density of N_2^+ ions,

$$X(t_1) = \int_{t_0}^{t_1} n_e(t) dt, \quad (7)$$

and

$$Y(t_i) = t_i - t_0. \quad (8)$$

As $n_{N_2}(t_i)$, $X(t_i)$ and $Y(t_i)$ are measured in the present experiments (or may be calculated from the measured quantities), we find the parameters $n_{N_2}(t_0)$, α and τ that fulfill Eq. (6) in the least square sense.

As has been shown by Shapko *et al.*,⁴⁵ by measuring at the same time both electron and ion number densities, reliable recombination rate coefficients can be evaluated even at conditions when the studied ions are not dominant in the afterglow plasma. If N_2^+ ions in excited vibrational states are present in afterglow plasma, they can serve as a source of N_2^+ ($\nu = 0$) ions due to cooling. As the measured number density of N_2^+ ($\nu = 1$) is very small (see in the following text), we do not consider this effect in the data analysis.

IV. UNCERTAINTIES AND THEIR SOURCES

The statistical uncertainty of the ion number density determination is on the order of $1 \times 10^8 \text{ cm}^{-3}$, and its systematic uncertainty arises mainly from the uncertainty in the discharge column length (estimated as 10%) and in the used vibrational transition moments. While the statistical uncertainty of the electron number density is very small, the systematic uncertainty is largely given by the precision of the determination of the resonant frequency of the empty cavity and is estimated to be less than $1 \times 10^8 \text{ cm}^{-3}$. The overall systematic uncertainty of the effective recombination rate coefficient determination is estimated to be 15%.

V. RESULTS AND DISCUSSION

An example of measured absorption line profiles (the dependence of absorbance divided by discharge column length on wavenumber) is shown in Fig. 2. The $P_{21}(10.5)$ and $Q_{22}(9.5)$ lines of the ${}^2\Sigma_g^+ - {}^2\Pi_u(0-2)$ band of N_2^+ are accompanied by a N_2 line around 12731.75 cm^{-1} . For recombination rate coefficient determination, only those N_2^+ lines that were not overlapping with N_2 lines were used. In this, we were aided by the list of wavelengths and relative intensities of molecular nitrogen transitions reported by Western *et al.*⁵⁴

The total number density of N_2^+ ions in $\nu = 0$ state was determined from the population of single state under the assumption of thermal populations of rotational levels. The $Q_{22}(9.5)$ transition was used in the majority of cases. A similar procedure was employed for the determination of the total number density of N_2^+ ions in $\nu = 1$ vibrational state. The dependence of relative number densities of N_2^+ ions in different rotational states of the vibrational ground state on rotational energy measured at $T_H = 139 \pm 3 \text{ K}$ is plotted in Fig. 3. The statistical weight of each state was taken into account. The obtained rotational temperature was $T_{\text{rot}} = 136 \pm 5 \text{ K}$, a value very close to T_H . As the number density of the probed rotational states of vibrationally excited N_2^+ ions was very low, we assumed that the populations of rotational states for N_2^+ ($\nu = 1$) are in accordance with thermal equilibrium at a given temperature.

An example of absorption line profiles for transitions originating in the ground and the first excited vibrational states of N_2^+ is shown in Fig. 4. Under assumption of thermal population of rotational energy levels in $\nu = 1$ state, only 1.5% of all N_2^+ ions

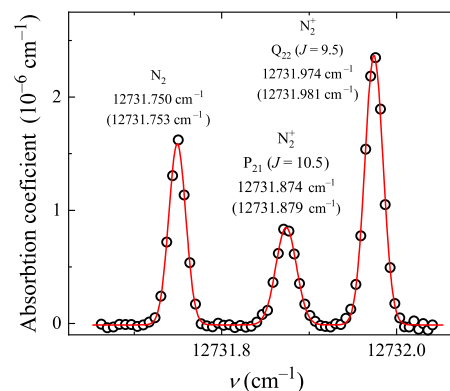


FIG. 2. Example of spectra measured around 12732 cm^{-1} in discharge plasma. Each line is labeled by the name of the corresponding species (N_2 or N_2^+), spectroscopic notation of the transition, and the measured central wavelength. The numbers in parentheses are wavenumbers from Refs. 51 and 54. The data were obtained at $T_H = 209 \text{ K}$, $[He] = 7 \times 10^{16} \text{ cm}^{-3}$ and $[N_2] = 7 \times 10^{14} \text{ cm}^{-3}$.

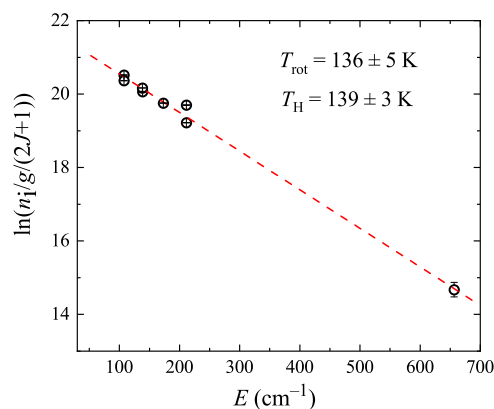


FIG. 3. The dependence of the relative number densities of N_2^+ ions in different rotational states of the ground vibrational state on the energy of given state (Boltzmann plot). J denotes the rotational quantum number and g the nuclear spin degeneracy factor of the state with measured number density n_i . The data were obtained in discharge plasma. The obtained rotational temperature $T_{\text{rot}} = 136 \pm 5 \text{ K}$ is very close to the temperature of the discharge tube holder $T_H = 139 \pm 3 \text{ K}$. The helium and N_2 number densities were 1.0×10^{17} and $5.5 \times 10^{14} \text{ cm}^{-3}$, respectively.

are in the first vibrationally excited state. This corresponds to the vibrational temperature of $\sim 750 \text{ K}$. By changing the experimental conditions (discharge power, reactant, and buffer gas number densities), we were able to slightly increase the relative population of the $\nu = 1$ state. The highest fraction was obtained when neon buffer gas was used instead of helium—around 3% of all ions were in $\nu = 1$ state. The measured recombination rate coefficient at such conditions was $\alpha(200 \text{ K}) = (3.0 \pm 0.3) \times 10^{-7} \text{ cm}^3 \text{ s}^{-1}$. In the following text, only the results of experiments conducted in helium buffer gas and with the lowest vibrational excitation of the ions will be presented.

Typical time evolutions of electron and N_2^+ number densities measured in afterglow plasma are shown in Fig. 5. The measured

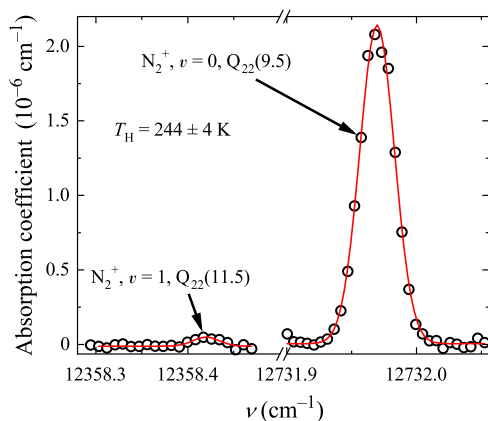
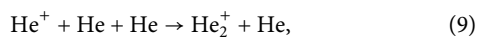
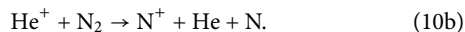
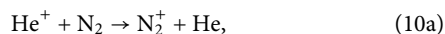


FIG. 4. Comparison of absorption line profiles of two lines originating in the ground and the first excited vibrational state of N_2^+ . The data were obtained in discharge at temperature of the discharge tube holder $T_H = 244 \pm 4$ K, $[He] = 5.8 \times 10^{16} \text{ cm}^{-3}$ and $[N_2] = 1.0 \times 10^{15} \text{ cm}^{-3}$. The calculated amount of vibrationally excited N_2^+ in the discharge is 1.5% of all N_2^+ ions.

number density of N_2^+ ions is lower than the electron number density and the relative fraction of N_2^+ with respect to all ions decreases at later times in the afterglow. Part of this behavior is due to the formation of N_4^+ ions in the three-body association reaction of N_2^+ with helium and molecular nitrogen (5). In order to minimize the influence of process (5) on plasma decay we had to keep the helium buffer gas density quite low—below $1 \times 10^{17} \text{ cm}^{-3}$. At such conditions, the He^+ ions formed in the discharge are not converted sufficiently fast to He_2^+ ions in three-body association reaction,



and may remain in the afterglow plasma. The value of the rate coefficient for reaction (9) was reported to be $1 \times 10^{-31} \text{ cm}^6 \text{ s}^{-1}$ at 300 K.⁵⁵ After switching off the discharge, He^+ ions are quickly removed from the afterglow plasma by a fast ion-molecule reaction with N_2 :



Reactions (10a) and (10b) slightly favor production of N^+ ions over N_2^+ .⁵⁶ A subsequent three-body association reaction of N^+ ions with helium and N_2 then leads to formation of N_3^+ ions. The reported experiments were aided by a model of chemical kinetics that included the main processes influencing charged particles in afterglow plasma. The model is further described in Appendix.

A crucial parameter for recombination studies is the electron temperature. In helium buffered stationary afterglow plasma, metastable electronic states of helium (2^1S and 2^3S) are formed in the discharge and can in superelastic collisions transfer energy to electrons thus increasing the electron temperature.⁵⁷ In the present experiments, the helium metastable atoms He^m are removed from the afterglow plasma by Penning ionization of N_2 :

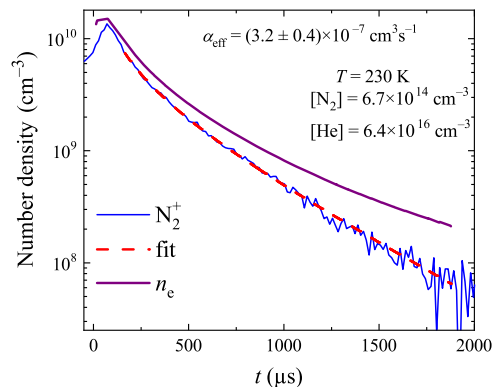
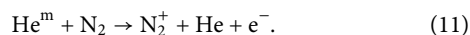


FIG. 5. Time evolution of the measured electron and N_2^+ number densities obtained at 230 K. The buffer gas and reactant number densities were: $[He] = 6.4 \times 10^{16} \text{ cm}^{-3} \text{ s}^{-1}$ and $[N_2] = 6.7 \times 10^{14} \text{ cm}^{-3} \text{ s}^{-1}$. The dashed line denotes fit of the data by Eq. (6). The N_2^+ number density was calculated from the absorbance at the center of the $Q_{22}(9.5)$ transition of the ${}^2\Sigma_g^+ - {}^2\Pi_u(0-2)$ band of N_2^+ under the assumption of thermal population of rotational states. Time is set to zero at the beginning of the afterglow.

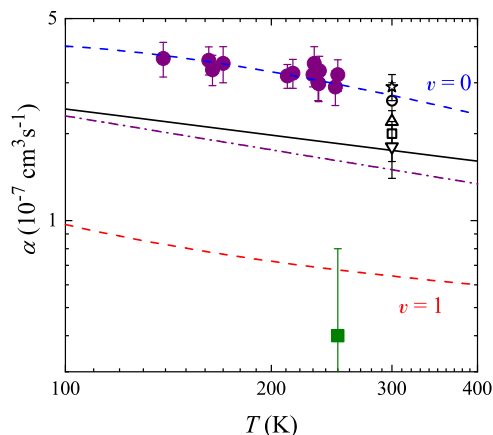


FIG. 6. The dependence of N_2^+ recombination rate coefficient on temperature. Present data (full circles: $v = 0$ state; full square: rate coefficient inferred for ions in vibrationally excited states and assumed to be close to the value pertaining to the $v = 1$ state, see in text) are compared with the results of recent quantum mechanical calculations by Abdoulanziz *et al.*⁴³ for particular vibrational states (dashed lines denoted $v = 0$ and $v = 1$). Values obtained in previous experiments by Peterson *et al.*,³⁶ Sheehan and St-Maurice,¹³ Zipf,²⁶ Canosa *et al.*,³¹ Kasner and Biondi,²⁴ Mehr and Biondi,²⁵ and Geoghegan *et al.*³⁰ are plotted as full line, dashed-dotted line, up triangle, circle, star, down triangle and open square, respectively.

We estimated the reaction rate coefficient for Penning ionization of N_2 in collisions with helium metastable atoms (11) from the increase of electron and N_2^+ number densities in the early afterglow at given temperature and N_2 number densities. As the time evolution of the number density of the helium metastable atoms was not directly measured and we have to roughly estimate the electron and

TABLE II. Comparison of values of recombination rate coefficient for N_2^+ ions obtained in present and in previous experiments with available information on N_2^+ vibrational excitation. The recombination rate coefficients from Refs. 13 and 36 are stated to be valid for electron temperature T_e lower than 1200 K. The present data were obtained in the temperature range of 140–250 K.

Reference	$\nu = 0$ (%)	$\nu = 1$ (%)	$\nu = 2$ (%)	$\nu = 3$ (%)	α ($10^{-7} \text{ cm}^3 \text{ s}^{-1}$)
36 ^a	46	27	10	16	$(1.75 \pm 0.09) \times (T_e/300)^{-0.30}$
13 ^b	65.1	21.1	8.4	3.5	$(1.5 \pm 0.23) \times (T_e/300)^{-0.38}$
26	87	11	2		2.2 at 300 K
Present ^c	98.5	1.5			$(2.95 \pm 0.50) \times (T/300)^{-0.28 \pm 0.07}$

^aIndicated rate coefficient was recalculated by Sheehan and St.-Maurice¹³ to be $\alpha = (1.50 \pm 0.23) \times (T_e/300)^{-0.39} \times (10^{-7} \text{ cm}^3 \text{ s}^{-1})$.

^bVibrational populations were estimated based on the calculations in Ref. 35.

^cFit of the data plotted in Fig. 6.

ion loss processes in the early afterglow, such an approach is inherently burdened by a large systematic error. The inferred reaction rate coefficients for Penning ionization of N_2 by helium metastable atoms were $k^m(140 \text{ K}) = (3_{-1.5}^{+3}) \times 10^{-11} \text{ cm}^3 \text{ s}^{-1}$ and $k^m(250 \text{ K}) = (5_{-2.5}^{+5}) \times 10^{-11} \text{ cm}^3 \text{ s}^{-1}$. This is in reasonable agreement with the previous measurement by Lindinger *et al.*⁵⁸ who reported a value of $k^m(300 \text{ K}) = 7 \times 10^{-11} \text{ cm}^3 \text{ s}^{-1}$.

In our study of N_2^+ recombination, we kept the number density of N_2 sufficiently high to ensure that helium metastable atoms are removed from the afterglow plasma within 100 μs after switching off the discharge. The data obtained within the first 200 μs of the afterglow are excluded from the data analysis.

The values of recombination rate coefficients obtained in the temperature range of 140–250 K are plotted in Fig. 6 and compared with the results from previous experimental and theoretical studies. Our results are in an excellent agreement with recent theoretical predictions for N_2^+ ($\nu = 0$) by Abdoulanziz *et al.*⁴³ The values of recombination rate coefficient obtained by other groups who also monitored the vibrational state of recombining ions are substantially lower than our data. In all these experiments, a large fraction of ions was vibrationally excited. This indicates, in agreement with analysis by Bates and Mitchell²⁸ and Sheehan and St.-Maurice¹³ that the recombination process is less efficient for vibrationally excited ions than for the ground vibrational state of N_2^+ . A summary of previous studies that probed populations of vibrational levels of N_2^+ ions is given in Table II.

By taking together available experimental data from Table II, we can make an estimate of the recombination rate coefficient for higher vibrational states. As the available state resolved experimental data are very scarce, we were unable to calculate the recombination rate coefficient for particular state with sufficient precision. Instead, we fitted the recombination rate coefficients from Table II with the following equation:

$$\alpha(f_0, f_1, f_2, f_3, T) = \alpha_{\nu=0}(T)f_0 + \alpha_{\nu>0}(T)(f_1 + f_2 + f_3), \quad (12)$$

where $\alpha(f_0, f_1, f_2, f_3, T)$ are the recombination rate coefficients from Table II, f_i are the fractional vibrational populations of N_2^+ ions for given vibrational state with $\nu = i$, $\alpha_{\nu=0}$ is the recombination rate coefficient for the ground vibrational state and $\alpha_{\nu>0}$ is the effective recombination rate coefficient for N_2^+ ions with $\nu > 0$.

The value of the recombination rate coefficient reported by Zipf²⁶ was obtained at 300 K. We extrapolated this value to 250 K using temperature dependence observed by Mehr and Biondi,²⁵ which is exactly the same as the one measured in single-pass merged electron-ion beam experiment by Sheehan and St.-Maurice.¹³

In the fitting procedure, we used the present experimental data in place of $\alpha_{\nu=0}$ as majority of the ions were in $\nu = 0$ state. The resulting effective recombination rate coefficient was $\alpha_{\nu>0} = (4 \pm 4) \times 10^{-8} \text{ cm}^3 \text{ s}^{-1}$ at 250 K. As in all experiments listed in Table II the majority of vibrationally excited ions were in $\nu = 1$ state, we assume that the obtained value will be close to the recombination rate coefficient for that state. The theoretical calculations by Abdoulanziz *et al.*⁴³ predicted value of $\alpha_{\nu=1} = 6.8 \times 10^{-8} \text{ cm}^3 \text{ s}^{-1}$ for the first excited vibrational state of N_2^+ . This is in a good agreement with our results.

Note that the vibrational populations reported for single-pass merged electron-ion beam experiment by Sheehan and St.-Maurice¹³ were not measured *in situ* but estimated based on calculations in Ref. 35. The vibrational populations obtained in ion storage ring experiment CRYRING³⁶ are, in fact, convoluted with the state specific rates of the dissociative recombination. We did not account for unknown uncertainties of these vibrational populations in our data analysis.

VI. SUMMARY

We have studied the recombination of N_2^+ ions, predominantly in their ground vibrational state, with electrons in the temperature range of 140–250 K. The results are in good agreement with the most recent quantum mechanical calculations.⁴³ By comparing our data to the recombination rate coefficients obtained by other groups with higher vibrational excitation of N_2^+ ions, we inferred that N_2^+ ions in the first excited vibrational state recombine with electrons less efficiently than the ions in the vibrational ground state. The recommended value of recombination rate coefficient for recombination of N_2^+ ($\nu = 0$) ions with electrons is $\alpha_{\nu=0} = (2.95 \pm 0.50) \times 10^{-7} (300/T)^{0.28 \pm 0.07} \text{ cm}^3 \text{ s}^{-1}$ in the range of 140–250 K and for N_2^+ ($\nu = 1$), $\alpha_{\nu=1} = (4 \pm 4) \times 10^{-8} \text{ cm}^3 \text{ s}^{-1}$ at 250 K.

We hope that our results will help to improve models of nitrogen containing planetary ionospheres and of nitrogen plasmas in general.

TABLE III. The most important reactions for the formation and destruction of N_2^+ ions included in the model of chemical kinetics. The ambipolar diffusion losses were calculated for $T = 230$ K. The characteristic reaction times were calculated using the formula: $\tau = 1/k[R]$, where k is the rate coefficient of the reaction, $[R]$ is the neutral reactant number density for the two body reactions, and the product of the neutral reactant number densities for the three body reactions. The number densities used in the model were $[He] = 6.4 \times 10^{16} \text{ cm}^{-3}$ and $[N_2] = 6.7 \times 10^{14} \text{ cm}^{-3}$.

No.	Reaction	Rate coefficient (cm^{-3}), ($\text{cm}^6 \text{ s}^{-1}$)	Characteristic reaction time (s)	Reference
R1	$\text{He}^m + \text{N}_2 \rightarrow \text{N}_2^+ + \text{He} + e^-$	6.1×10^{-11}	2.45×10^{-5}	58, 230 K
R2	$\text{He}^+ + \text{He} + \text{He} \rightarrow \text{He}_2^+ + \text{He}$	1.0×10^{-31}	2.44×10^{-3}	61
R3	$\text{He}_2^+ + \text{N}_2 \rightarrow \text{N}_2^+ + \text{He} + \text{He}$	1.12×10^{-9}	1.33×10^{-6}	58
R4	$\text{N}^+ + \text{N}_2 + \text{He} \rightarrow \text{N}_3^+ + \text{He}$	2.0×10^{-29}	5.83×10^{-4}	53
R5	$\text{N}^+ + \text{N}_2 + \text{N}_2 \rightarrow \text{N}_3^+ + \text{N}_2$	8.0×10^{-29}	2.59×10^{-1}	53
R6	$\text{He}^+ + \text{N}_2 \rightarrow \text{N}^+ + \text{He} + \text{N}$	8.4×10^{-10}	1.77×10^{-6}	56
R7	$\text{He}^+ + \text{N}_2 \rightarrow \text{N}_2^+ + \text{He}$	6.6×10^{-10}	2.26×10^{-6}	56
R8	$\text{N}_2^+ + \text{N}_2 + \text{He} \rightarrow \text{N}_4^+ + \text{He}$	2.0×10^{-29}	1.23×10^{-3}	53
R9	$\text{N}_2^+ + \text{N}_2 + \text{N}_2 \rightarrow \text{N}_4^+ + \text{N}_2$	8.0×10^{-29}	2.78×10^{-2}	53
R10	$\text{N}_2^+ + e^- \rightarrow \text{N} + \text{N}$	3.5×10^{-7}	1.90×10^{-4}	Present data
R11	$\text{N}_3^+ + e^- \rightarrow \text{N}_2 + \text{N}$	6.5×10^{-7}	1.03×10^{-4}	62
R12	$\text{N}_4^+ + e^- \rightarrow \text{N}_2 + \text{N}_2$	2.3×10^{-6}	2.56×10^{-5}	63
R13	N_2^+ ambipolar diffusion		6.50×10^{-4}	64

ACKNOWLEDGMENTS

This work was partly supported by the Czech Science Foundation (Grant Nos. GACR 23-05439S and GACR 22-05935S) and by the Charles University (Grant Nos. GAUK 337821 and GAUK 332422).

AUTHOR DECLARATIONS

Conflict of Interest

The authors have no conflicts to disclose.

Author Contributions

L. Uvarova: Conceptualization (lead); Data curation (equal); Formal analysis (equal); Funding acquisition (equal); Investigation (equal); Methodology (equal); Project administration (lead); Supervision (lead); Writing – original draft (equal); Writing – review & editing (equal). **S. Rednyk:** Data curation (equal); Investigation (equal); Software (equal); Writing – review & editing (equal). **P. Dohnal:** Conceptualization (lead); Data curation (equal); Formal analysis (equal); Funding acquisition (equal); Investigation (equal); Methodology (equal); Project administration (lead); Software (equal); Supervision (lead); Writing – original draft (equal); Writing – review & editing (equal). **M. Kassayová:** Formal analysis (equal); Funding acquisition (equal); Investigation (equal); Writing – review & editing (equal). **S. Saito:** Formal analysis (equal); Investigation (equal). **Š. Roučka:** Formal analysis (equal); Software (equal); Visualization (equal); Writing – review & editing (equal). **R. Plašil:** Data curation (equal); Software (equal); Supervision (equal); Writing – review & editing (equal). **R. Johnsen:** Conceptualization (supporting); Writing – original draft (equal); Writing – review & editing (equal). **J. Glosík:** Conceptualization (supporting); Funding acquisition (equal); Methodology (equal); Writing – review & editing (equal).

sition (equal); Methodology (equal); Writing – review & editing (equal).

DATA AVAILABILITY

The data that support the findings of this study are available from the corresponding author upon reasonable request.

APPENDIX: MODEL OF CHEMICAL KINETICS

A kinetic model was used in the experiment for prediction of the chemical evolution of the afterglow plasma with conditions similar to the experiment. The model was based on the set of reaction equations of binary or ternary interactions of ions, electrons, and neutrals with corresponding rate coefficients. The model also included the ambipolar diffusion with corresponding characteristic time of the charged particles losses. Differential equations of the kinetic model were solved by using an equation solver implemented in Isoda routine.⁵⁹ The chemical reactions used in the kinetic model are summarized in Table III. The temperature for the reaction rate coefficients in Table III is 300 K if not stated otherwise.

Based on experimental study by Glosik *et al.*,⁶⁰ we have presumed, that the number density of metastable helium atoms He^m for both 2^1S and 2^3S states was the same or lower than the electron number density at the beginning of the afterglow. The rate coefficient for reaction R1 was obtained from Lindinger, Schmeltekopf, and Fehsenfeld⁵⁸ by extrapolating the published temperature dependence to 230 K.

The actual ionic composition at the beginning of the afterglow was not known – with the exception of N_2^+ ions and electrons that were probed in the experiment. Various initial compositions of ions were tried for the kinetic model, until an agreement with the experiment was achieved.

The comparison between the measured number densities of N_2^+ and of electrons and number densities obtained from kinetic model

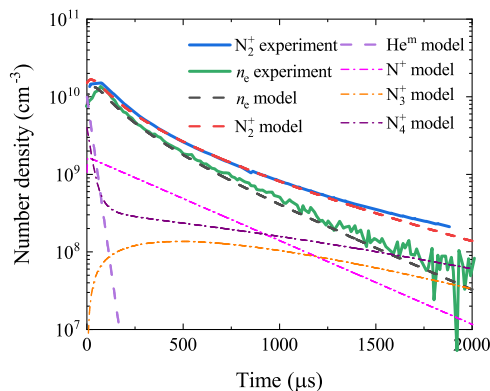


FIG. 7. The time evolution of the measured number densities of N_2^+ and electrons and of the number densities obtained from the model of chemical kinetics at $T = 230$ K.

of the afterglow is shown in Fig. 7. Both, the kinetic model as well as the measured data were obtained at temperature of $T = 230$ K. The kinetic model shows that the formation of N_2^+ ions is finished within $250 \mu\text{s}$ after switching off the discharge in good agreement with the measured data.

REFERENCES

- V. A. Krasnopolsky, "A photochemical model of Pluto's atmosphere and ionosphere," *Icarus* **335**, 113374 (2020).
- V. A. Krasnopolsky, "Chemical composition of Titan's atmosphere and ionosphere: Observations and the photochemical model," *Icarus* **236**, 83–91 (2014).
- J. Elliot, D. Strobel, X. Zhu, J. Stansberry, L. Wasserman, and O. Franz, "The thermal structure of Triton's middle atmosphere," *Icarus* **143**, 425–428 (2000).
- L. A. Young, F. Braga-Ribas, and R. E. Johnson, "Chapter 6—Volatile evolution and atmospheres of trans-Neptunian objects," in *The Trans-Neptunian Solar System*, edited by D. Prrialnik, M. A. Barucci, and L. A. Young (Elsevier, 2020), pp. 127–151.
- M.-Y. Lin and R. Ilie, "A review of observations of molecular ions in the Earth's magnetosphere-ionosphere system," *Front. Astron. Space Sci.* **8**, 745357 (2022).
- H. Lammer, W. Stumptner, G. J. Molina-Cuberos, S. J. Bauer, and T. Owen, "Nitrogen isotope fractionation and its consequence for Titan's atmospheric evolution," *Planet. Space Sci.* **48**, 529–543 (2000).
- Y. L. Yung and J. R. Lyons, "Triton: Topside ionosphere and nitrogen escape," *Geophys. Res. Lett.* **17**, 1717–1720, <https://doi.org/10.1029/g1017i010p01717> (1990).
- M. Sharma and B. Saikia, "Discharge conditions and emission spectroscopy of N_2 and N_2^+ active species in a variable power dc pulsed plasma used for steel nitriding," *Indian J. Pure Appl. Phys.* **46**, 370–463 (2008).
- I. A. Morozov, A. S. Mamaev, I. V. Osorgina, L. M. Lemkina, V. P. Korobov, A. Y. Belyaev, S. E. Porozova, and M. G. Sherban, "Structural–mechanical and antibacterial properties of a soft elastic polyurethane surface after plasma immersion N_2^+ implantation," *Mater. Sci. Eng.: C* **62**, 242–248 (2016).
- T. Sakakura, N. Murakami, Y. Takatsuji, M. Morimoto, and T. Haruyama, "Contribution of discharge excited atomic N, N_2 , and N_2^+ to a plasma/liquid interfacial reaction as suggested by quantitative analysis," *Eur. J. Chem. Phys. Phys. Chem.* **20**, 1467–1474 (2019).
- J. D. Holcomb and A. Schucker, "Helium plasma skin regeneration: Evaluation of skin tissue effects in a porcine model and comparison to nitrogen plasma skin regeneration," *Lasers Surg. Med.* **52**, 23–32 (2020).
- J. L. Fox and A. Dalgarno, "The vibrational distribution of N_2^+ in the terrestrial ionosphere," *J. Geophys. Res.: Space Phys.* **90**, 7557–7567, <https://doi.org/10.1029/ja090ia08p07557> (1985).
- C. H. Sheehan and J.-P. St.-Maurice, "Dissociative recombination of N_2^+ , O_2^+ , and NO^+ : Rate coefficients for ground state and vibrationally excited ions," *J. Geophys. Res.: Space Phys.* **109**, A03302, <https://doi.org/10.1029/2003ja010132> (2004).
- J. L. Fox, "Effects of dissociative recombination on the composition of planetary atmospheres," *J. Phys.: Conf. Ser.* **4**, 32–37 (2005).
- A. Florescu-Mitchell and J. Mitchell, "Dissociative recombination," *Phys. Rep.* **430**, 277–374 (2006).
- M. Larsson and A. E. Orel, *Dissociative Recombination of Molecular Ions*, Cambridge Molecular Science (Cambridge University Press, 2008).
- Y. Chen, L. Liu, H. Le, and H. Zhang, "Latitudinal dependence of daytime electron density bite-out in the ionospheric F_2 -layer," *J. Geophys. Res.: Space Phys.* **126**, e2020JA028277, <https://doi.org/10.1029/2020ja028277> (2021).
- W. J. McNeil, R. A. Dressler, and E. Murad, "Impact of a major meteor storm on Earth's ionosphere: A modeling study," *J. Geophys. Res.: Space Phys.* **106**, 10447–10465, <https://doi.org/10.1029/2000ja000381> (2001).
- K. Schlegel, "Reduced effective recombination coefficient in the disturbed polar E -region," *J. Atmos. Terr. Phys.* **44**, 183–185 (1982).
- L. M. Kagan and M. C. Kelley, "A thermal mechanism for generation of small-scale irregularities in the ionospheric E region," *J. Geophys. Res.: Space Phys.* **105**, 5291–5303, <https://doi.org/10.1029/1999ja000415> (2000).
- M.-Y. Chou, I. Chorniak, C. C. Lin, and N. Pedatella, "The persistent ionospheric responses over Japan after the impact of the 2011 Tohoku earthquake," *Space Weather* **18**, e2019SW002302, <https://doi.org/10.1029/2019sw002302> (2020).
- M. A. Biondi and S. C. Brown, "Measurement of electron-ion recombination," *Phys. Rev.* **76**, 1697–1700 (1949).
- D. R. Bates, "Dissociative recombination," *Phys. Rev.* **78**, 492–493 (1950).
- W. H. Kasner and M. A. Biondi, "Electron-ion recombination in nitrogen," *Phys. Rev.* **137**, A317–A329 (1965).
- F. J. Mehr and M. A. Biondi, "Electron temperature dependence of recombination of O_2^+ and N_2^+ ions with electrons," *Phys. Rev.* **181**, 264–271 (1969).
- E. C. Zipf, "The dissociative recombination of vibrationally excited N_2^+ ions," *Geophys. Res. Lett.* **7**, 645–648, <https://doi.org/10.1029/g1007i009p00645> (1980).
- R. Johnsen, "Microwave afterglow measurements of the dissociative recombination of molecular ions with electrons," *Int. J. Mass Spectrom. Ion Processes* **81**, 67–84 (1987).
- D. R. Bates and J. B. A. Mitchell, "Rate coefficients for $N_2^+(v)$ dissociative recombination," *Planet. Space Sci.* **39**, 1297–1300 (1991).
- M. R. Mahdavi, J. B. Hasted, and M. M. Nakshbandi, "Electron-ion recombination measurements in the flowing afterglow," *J. Phys. B: At. Mol. Phys.* **4**, 1726–1737 (1971).
- M. Geoghegan, N. G. Adams, and D. Smith, "Determination of the electron-ion dissociative recombination coefficients for several molecular ions at 300 K," *J. Phys. B: At. Mol. Opt. Phys.* **24**, 2589–2599 (1991).
- A. Canosa, J. C. Gomet, B. R. Rowe, and J. L. Queffelec, "Flowing afterglow Langmuir probe measurement of the $N_2^+(v=0)$ dissociative recombination rate coefficient," *J. Chem. Phys.* **94**, 7159–7163 (1991).
- A. J. Cunningham and R. M. Hobson, "Dissociative recombination at elevated temperatures. IV. N_2^+ dominated afterglows," *J. Phys. B: At. Mol. Phys.* **5**, 2328–2331 (1972).
- P. M. Mul and J. W. McGowan, "Merged electron-ion beam experiments. III. temperature dependence of dissociative recombination for atmospheric ions NO^+ , O_2^+ , N_2^+ ," *J. Phys. B: At. Mol. Phys.* **12**, 1591–1601 (1979).
- J. Brian and A. Mitchell, "The dissociative recombination of molecular ions," *Phys. Rep.* **186**, 215–248 (1990).
- C. Noren, F. B. Yousif, and J. B. A. Mitchell, "Dissociative recombination and excitation of N_2^+ ," *J. Chem. Soc., Faraday Trans. 2* **85**, 1697–1703 (1989).
- J. R. Peterson, A. Le Padellec, H. Danared, G. H. Dunn, M. Larsson, A. Larson, R. Peverall, C. Strömholm, S. Rosén, M. af Ugglas, and W. J. van der Zande, "Dissociative recombination and excitation of N_2^+ : Cross sections and product branching ratios," *J. Chem. Phys.* **108**, 1978–1988 (1998).

- ³⁷S. L. Guberman, "Dissociative recombination of the ground state of N_2^+ ," *Geophys. Res. Lett.* **18**, 1051–1054, <https://doi.org/10.1029/91gl01157> (1991).
- ³⁸S. L. Guberman, "Role of excited core Rydberg states in dissociative recombination," *J. Phys. Chem. A* **111**, 11254–11260 (2007).
- ³⁹S. L. Guberman, "Spectroscopy above the ionization threshold: Dissociative recombination of the ground vibrational level of N_2^+ ," *J. Chem. Phys.* **137**, 074309 (2012).
- ⁴⁰S. L. Guberman, "The vibrational dependence of dissociative recombination: Cross sections for N_2^+ ," *J. Chem. Phys.* **139**, 124318 (2013).
- ⁴¹S. L. Guberman, "The vibrational dependence of dissociative recombination: Rate constants for N_2^+ ," *J. Chem. Phys.* **141**, 204307 (2014).
- ⁴²D. A. Little, K. Chakrabarti, J. Z. Mezei, I. F. Schneider, and J. Tennyson, "Dissociative recombination of N_2^+ : An *ab initio* study," *Phys. Rev. A* **90**, 052705 (2014).
- ⁴³A. Abdoulanziz, C. Argentin, V. Laporta, K. Chakrabarti, A. Bultel, J. Tennyson, I. F. Schneider, and J. Z. Mezei, "Low-energy electron impact dissociative recombination and vibrational transitions of N_2^+ ," *J. Appl. Phys.* **129**, 053303 (2021).
- ⁴⁴R. Plašil, P. Dohnal, Á. Kálosi, Š. Roučka, D. Shapko, S. Rednyk, R. Johnsen, and J. Glosík, "Stationary afterglow apparatus with CRDS for study of processes in plasmas from 300 K down to 30 K," *Rev. Sci. Instrum.* **89**, 063116 (2018).
- ⁴⁵D. Shapko, P. Dohnal, Š. Roučka, L. Uvarova, M. Kassayová, R. Plašil, and J. Glosík, "Cavity ring-down spectroscopy study of neon assisted recombination of H_3^+ ions with electrons," *J. Mol. Spectrosc.* **378**, 111450 (2021).
- ⁴⁶D. Romanini, A. A. Kachanov, N. Sadeghi, and F. Stoeckel, "CW cavity ring down spectroscopy," *Chem. Phys. Lett.* **264**, 316–322 (1997).
- ⁴⁷Z. Qin, J. M. Zhao, and L. H. Liu, "Radiative transition probabilities for the main diatomic electronic systems of N_2 , N_2^+ , NO, O_2 , CO_2^+ , CO^+ , CN_2^+ , C_2 and H_2 produced in plasma of atmospheric entry," *J. Quant. Spectrosc. Radiat. Transfer* **202**, 286–301 (2017).
- ⁴⁸L. S. Rothman, C. P. Rinsland, A. Goldman, S. T. Massie, D. P. Edwards, J.-M. Flaud, A. Perrin, C. Camy-Peyret, V. Dana, J.-Y. Mandin, J. Schroeder, A. Mccann, R. R. Gamache, R. B. Wattson, K. Yoshino, K. V. Chance, K. W. Jucks, L. R. Brown, V. Nemtchinov, and P. Varanasi, "The HITRAN molecular spectroscopic database and HAWKS (HITRAN atmospheric workstation): 1996 edition," *J. Quant. Spectrosc. Radiat. Transfer* **60**, 665–710 (1998).
- ⁴⁹A. Hansson and J. K. G. Watson, "A comment on Hönl-London factors," *J. Mol. Spectrosc.* **233**, 169–173 (2005).
- ⁵⁰L. T. Earls, "Intensities in ${}^2\Pi-{}^2\Sigma$ transitions in diatomic molecules," *Phys. Rev.* **48**, 423–424 (1935).
- ⁵¹Y.-d. Wu, J.-w. Ben, L. Li, L.-j. Zheng, Y.-q. Chen, and X.-h. Yang, "Study of (2, 0) band of $A_u^2-X_g^{2+}$ system of N_2^+ by optical heterodyne detected velocity modulation spectroscopy," *Chin. J. Chem. Phys.* **20**, 285–290 (2007).
- ⁵²W. Benesch, D. Rivers, and J. Moore, "High resolution spectrum of the N_2^+ Meinel system to 11 250 Å," *J. Opt. Soc. Am.* **70**, 792–799 (1980).
- ⁵³V. Anicich, D. B. Milligan, D. A. Fairley, and M. J. McEwan, "Termolecular ion-molecule reactions in Titan's atmosphere, I: Principal ions with principal neutrals," *Icarus* **146**, 118–124 (2000).
- ⁵⁴C. M. Western, L. Carter-Blatchford, P. Crozet, A. J. Ross, J. Morville, and D. W. Tokaryk, "The spectrum of N_2 from 4,500 to 15,700 cm^{-1} revisited with PGOPHER," *J. Quant. Spectrosc. Radiat. Transfer* **219**, 127–141 (2018).
- ⁵⁵Y. Ikezoe, S. Matsuoka, M. Takebe, and A. Viggiano, *Gas Phase Ion-Molecule Reaction Rate Constants Through 1986* (Maruzen Company Ltd., 1987).
- ⁵⁶K. R. Lane, "Flowing afterglow studies of gas-phase anionic transition-metal chemistry (nucleophilic addition, bond energies, oxidation, carbonyls)," Ph.D. thesis, Purdue University (1986).
- ⁵⁷R. Plašil, I. Korolov, T. Kotrik, P. Dohnal, G. Bano, Z. Donko, and J. Glosík, "Non-Maxwellian electron energy distribution function in He, He/Ar, He/Xe/ H_2 and He/Xe/ D_2 low temperature afterglow plasma," *Eur. Phys. J. D* **54**, 391–398 (2009).
- ⁵⁸W. Lindinger, A. L. Schmeltekopf, and F. C. Fehsenfeld, "Temperature dependence of de-excitation rate constants of $He(2^3S)$ by Ne, Ar, Xe, H_2 , N_2 , O_2 , NH_3 , and CO_2 ," *J. Chem. Phys.* **61**, 2890–2895 (1974).
- ⁵⁹A. C. Hindmarsh, in *Scientific Computing, IMACS Transactions on Scientific Computation*, edited by R. S. Stepleman (North-Holland, 1983), Vol. **1**, pp. 55–64.
- ⁶⁰J. Glosík, G. Bánó, R. Plašil, A. Luca, and P. Zakouřil, "Study of the electron ion recombination in high pressure flowing afterglow: Recombination of NH_4^+ + $(NH_3)_2^+$," *Int. J. Mass Spectrom.* **189**, 103–113 (1999).
- ⁶¹J. Glosík, P. Dohnal, P. Rubovič, Á. Kálosi, R. Plašil, Š. Roučka, and R. Johnsen, "Recombination of H_3^+ ions with electrons in He/ H_2 ambient gas at temperatures from 240 K to 340 K," *Plasma Sources Sci. Technol.* **24**, 065017 (2015).
- ⁶²V. Zhaunerchyk, W. D. Geppert, E. Vignen, M. Hamberg, M. Danielsson, M. Larsson, R. D. Thomas, M. Kaminska, and F. Österdahl, "Dissociative recombination study of N_3^+ : Cross section and branching fraction measurements," *J. Chem. Phys.* **127**, 014305 (2007).
- ⁶³S. F. Adams, C. A. DeJoseph, and J. M. Williamson, "Formation and electron-ion recombination of N_4^+ following photoionization in near-atmospheric pressure N_2 ," *J. Chem. Phys.* **130**, 144316 (2009).
- ⁶⁴L. A. Viehland and E. A. Mason, "Transport properties of gaseous ions over a wide energy range, IV," *At. Data Nucl. Data Tables* **60**, 37–95 (1995).